Energy Conversion and Management: X 20 (2023) 100437

Contents lists available at ScienceDirect

Energy Conversion and Management: X

journal homepage: www.sciencedirect.com/journal/energy-conversion-and-management-x

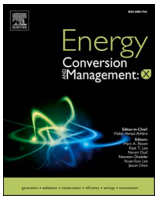

High-efficiency solution for an open-loop desiccant assisted solar cooling system by integrating *trans*-critical CO_2 heat pumps: A comprehensive techno-economic assessment

Gianluigi Lo Basso, Ali Mojtahed *, Lorenzo Mario Pastore, Livio De Santoli

Department of Astronautics Electric and Energy Engineering, Sapienza University of Rome, Italy

ARTICLE INFO

Keywords:
Desiccant solar cooling system
Trans-critical CO_2 heat pump
Building energy efficiency
Hybrid energy system
HVAC
Energy efficiency

ABSTRACT

Solar cooling systems are classified into open and closed loop cycles. The latter is superior in terms of reliability and commercialization. However, the former, due to unique features to provide sensible and latent cooling separately is still under development.

This work proposes a potential improvement in terms of energy performance in solar-assisted open loop cycles. The cooling system is composed of desiccant wheel, indirect evaporative coolers that require regeneration power. Such power is provided by a cutting-edge technology named *trans*-critical CO_2 heat pump, running mostly by photovoltaic modules. Four different configurations are dynamically simulated inside MATLAB SIMULINK environment for the year interval.

Based on the main simulation results, the renewable energy share of at least 50% for both electric and thermal is achieved. It could be increased up to 77% electric and 100% for thermal share. Furthermore, the parameters to optimize the cooling system performance are the heat pump COP, the recovery heat exchanger effectiveness, and the regeneration air mass flow rate. Generally, the innovative cooling system behaviour is affected by climate variations. Hence, the COP of the CO_2 heat pump is starting from 2.3, which could be improved up to 6.5. It is clearly higher than the available benchmark.

Introduction

Inside the building sector, roughly around half of the energy is consumed for the inner space heating and cooling which also corresponds to 40% of primary energy resources. According to International Energy Agency (IEA), by 2050, 6205 TWh of energy will be consumed to provide conditioned air which is a 35% increase [1]. Adding to this, the global strategies which limit carbon footprint as much as possible will open the room for new technologies that guarantee clean and environmentally friendly resources [2]. Inside the European Union, directives obligate all new construction from 2020 to be Near Zero Energy Building (NZEB) [3]. The Energy Performance of Building Directive (EPBD) indicates that the Member States shall ensure new buildings occupied and owned by public authorities must be NZEBs after December 31, 2018, and that all new buildings are NZEBs by December 31, 2020 [4]. One potential solution in the building sector would be to implement hybrid systems integrated with renewable resources [5–7]. To do so, optimizing the HVAC process inside the building plays a key role. Generally, the air conditioning system corresponds to latent and sensible loads. Sensible heat is considered as the amount of heat that needs to be removed to decrease the temperature of the room, while latent heat is dealing with the amount of moisture that could be produced by the human body or captured from the environment. Such moisture is needed to be removed in order to maintain the comfort zone [8].

In general, almost all well-known AC technologies feature a thermal process which is necessary for providing cooling effect. Solar thermal driven refrigeration systems gave attention since 1960 s due to the sustainable solution that they are offering. However, because of poor energy performance and expensive technologies, they were not competitive except in recent decades. Inside these systems, solar thermal energy is captured through solar collector units which is used to run a sorption process. Sorption process can be held as an open or close cycle. Absorption and adsorption cooling systems are two most important cycles regarding close loop systems. Desiccant systems are recognized as open sorption cycles [9–11]. In general, closed- loop technologies particularly absorption chiller have gained more attention due to the promising performance to provide sensible cooling effect [12]. The

* Corresponding author.
E-mail address: ali.mojtahed@uniroma1.it (A. Mojtahed).

https://doi.org/10.1016/j.ecmx.2023.100437
Received 18 May 2023; Received in revised form 8 August 2023; Accepted 9 August 2023
Available online 17 August 2023

Nomenclature

COP	Coefficient of performance [%]
EER	Energy efficiency ratio [%]
P	Power [kW]
q	specific heat [kJ/kg]
h	specific enthalpy [kJ/kg]
m	mass flow rate [kg/s]
v	Air velocity [m/s]
N	Air specific flow rate[m^3/person/s]
Pe	Number of persons
f	Air flowrate [l/s]
c_p	specific heat capacity at constant pressure[kJ/kg*K]
s	Specific entropy [kJ/kg*K]
w	Specific work [kJ/kg]
T	Temperature [°C]
η	Efficiency [%]
E	Electric energy consumption (kWh)
ε	Heat exchanger effectiveness
μ	Thermodynamic perfection factor
Q	Thermal energy consumption (kWh)
RH	Relative humidity [%]
X	Absolute humidity [g/kg]
ρ	Density [kg/m^3]
V	Volume [m^3]
A	Surface [m^2]
G	Specific normal radiation [W/m^2]

subscripts

th	thermal
reg	regeneration airflow
p	process airflow
ext	external
el	electric
ev	evaporator
cond	condenser
ihex	Internal heat exchanger
is	isentropic
mec	mechanical
gc	gas cooler
h	hot
c	cold
in	inlet
out	outlet
hum	humidifier
sol	solar
abs	absorption
avg	average
sys	system

abbreviations

PV	Photovoltaic
HVAC	Heating Ventilation and Air conditioning
DW	Desiccant wheel
DCS	Desiccant cooling system
TC	Trans-critical
RES	Renewable energy share
PES	Primary energy saving
HP	Heat Pump
DEC	Desiccant evaporative cooling
EH	Electric heater
ES	Energy storage
EC	Evaporative cooling
REG	Regeneration coils
IEC	Indirect evaporative cooling
SC	Solar collector
NZEB	Near-zero energy building

Multicriteria Economic index

ECO	Flow cash
FC	Investment
INV	Pay Back Period
PBP	intervention
int	Capital expenditure
CAPEX	Net present value
NPV	Internal rate of return
IRR	interest rate
i	

desiccant rotary wheel (DW) works on the principle of desiccant dehumidification and evaporative cooling. The unique merit they have is that the sensible and the latent heat can be processed separately [13,14]. Figs. 1 and 2 show the working principle of solar desiccant cooling system. The moisture removal from the air occurs due to the different water vapor pressure between the air and the sorbent. The dry sorbent has lower vapor pressure than air stream. By capturing the water content, its vapor pressure tends to increase. the vapor pressure is the function of relative humidity as well as temperature. As they increase, the pressure value rises until it surpasses the air pressure. At this point captured water contents are exhausted to the ambient and the sorbent is drained out. In order to start another sorption cycle, the sorbent needs to be cooled down and decrease the vapor pressure. In Fig. 1, the process from point two to three is known as regeneration which is carried out through an external resource. Such heat resources could be run by solar collectors integrated with a storage tank and a backup heater [8].

'The current work presents a hybrid solar-based cooling system that provides a cooling effect mostly from renewable resources. This novel solution is proposed to justify the application of desiccant cooling systems by improving the energy performance of such systems. A *trans*-critical CO_2 heat pump is used to provide regeneration power to complete the wheel's cycle. Theoretically, Heat pump systems operate better for heating purposes rather than cooling (COP is always higher than

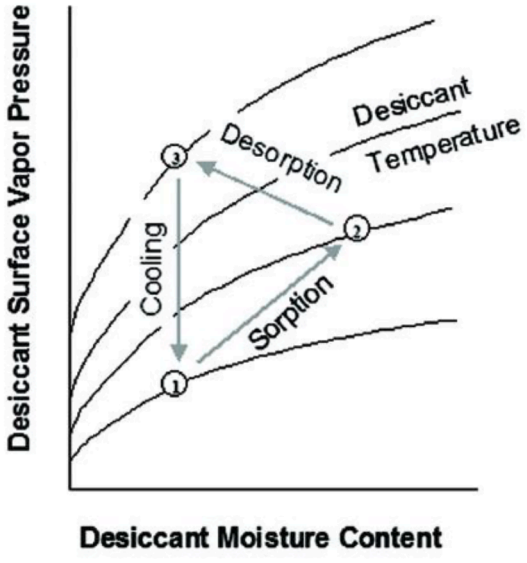

Fig. 1. Working principle of desiccant system.

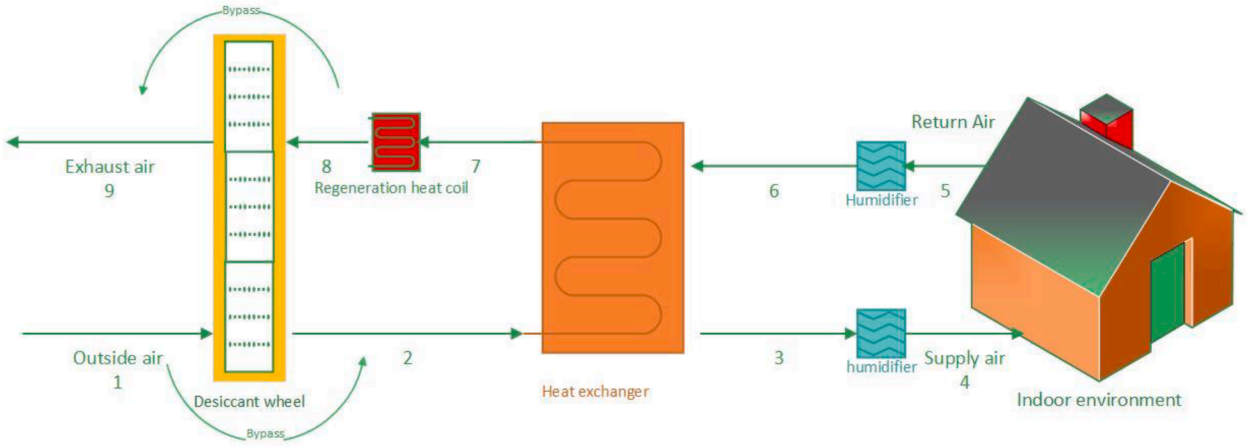

Fig. 2. Schematic of desiccant wheel system.

EER). As a result, the proposed configuration ensures higher energy performance respecting the same HP system that is used in a reverse cycle to provide a direct cooling effect.'

The layout is created inside the Revit environment and the load curve profile has been simulated for an annual period. After that, four different layouts are created and simulated dynamically by MATLAB SIMULINK tools. The common part of each layout remains desiccant wheel which run thermally by TC CO_2 HP.

Silica gel-type 1 is assumed as a desiccant material for those simulations [15–17].

The desiccant cooling system on literature

The desiccant-based cooling system has been the main subject of many research studies in the last two decades. Works in this area can be categorized into feasibility study, performance study and parametric analysis, as well as mathematical modelling [18].

Based on reports available in literature, the performance of desiccant cooling systems can be influenced by the climatic conditions, component performance, operating conditions, DW speed, airflow rate, and regeneration speed [19–21]. It is proved that desiccant cooling systems are fitted with humid climates due to their remarkable performance to provide latent cooling [22].

Other parametric designs like the impact of ambient conditions, demand conditions, and regeneration source type are studied by Sheng et al. [23]. He concluded that the rise of ambient temperature and humidity profile increases the wheel's performance. In other words, DW removes more water content from the air flow when the ambient is hot and humid.

In [23], the authors recognize regeneration temperature and outdoor humidity as more effective parameters to increase the performance rather than ambient temperature variation. It means in the same climate by varying regeneration temperature it is possible to improve the wheel's performance. Such results are carried out from experimental data.

To reach the higher COP values, two and multi-stage desiccant cooling layout are presented in [24] and [25] respectively. Moreover, the authors in [26] represented a precooling process prior to DW inlet as an useful parameter to improve COP.

Another interesting topic that has gained the attention was the integration of solar-based and hybrid cooling systems [27–29]. Solar energy exploitation is a good solution to provide heat requirement for the regeneration sector. The energy necessary for regeneration can be provided by solar collectors which are usually integrated with a storage tank to store the heat. Moreover, through heat exchangers such thermal energy can flow in the regeneration sector. In this way, use of solar thermal energy to supply a two-stage system consist of a traditional vapor compression cycle and desiccant wheel has been a subject of a work performed in Jiangsu, China [30] and [31] in Australia. In [32], the authors set up an experiment based on the solar thermal energy exclusively to be integrated with the regeneration sector of the liquid desiccant cooling system. Thermal storage is used to increase the capacity factor of the thermal energy. They studied solar fraction effectiveness as a parametric index to increase the size of thermal storage. In the work performed formerly by authors of this paper [33], the integration of solar collector with solid desiccant cooling system has already been carried out and the model has been used partially in this work as well.

Regarding mathematical simulation, several models are available in the literature [34–44], but in most cases, they are based on the detailed description of heat and mass transfers between air and desiccant material, utilizing partial differential equations. [45]. The complexity of such models short comes further progress in most cases. However, some works based on experimental results are available in which the mathematical equation is fitted according to experimental results. The main drawback of such an approach is diversion regarding desiccant material and temperature which dictates the correlation.

Beccali et al. [46] presented simple models to evaluate the performance of rotary wheels based on different kinds of solid desiccants. They presented "Model 54" which is developed for silica gel desiccant rotor. Such a model is based on experimental data and is used to predict outlet temperature and absolute humidity. It consists of 54 coefficients that correspond to each correlation for outlet absolute humidity and temperature. They stated that the model predicts very well the performance of the silica gel desiccant rotor (Type-I). Such result has been adapted as reference to simulate the DW unit in presented work.

Authors in [47], developed a dynamic model for solar cooling system in MATLAB- SIMULINK based on the existing case study of ENEA, research centre building in Rome. Another work using SIMULINK and TRNSYS [48], is performed to improve the efficiency of solar cooling system via optimized storage techniques and absorption chiller.

TC CO2 heat pump, working principle

CO_2 is one of the first natural refrigerants used in mechanical refrigeration systems. Yet, refrigerants like CFCs and HFCs were chosen over due to higher performance in cooling and heating space in previous decades. However, environmental concerns against using CFCs and HFCs have urged researchers to identify alternatives that are environmentally benign and can serve as an effective replacement to the conventionally used working fluids [49,50]. Among natural refrigerants, CO2 (ASHRAE safety class A1) is one of the few that is non-toxic and

non-flammable [51] and can be released to the environment without the need to be recovered from any dismissed equipment.

Despite its advantages, the two main issues that remain to deal with CO2 as a refrigerant are the low critical temperature (31.1 ℃) and high operating pressure (critical pressure 73.75 bar). To address the former, the cycle is designed to operate above the critical point. As a result, such a system is known as trans critical CO_2 heat pump (TC CO2 HP) in which the condenser is replaced by a gas cooler since no phase change takes place. It is found that the use of a gas cooler with heat rejection taking place over an unusually large temperature glide (100 – 120 ℃) offers several unique possibilities such as simultaneous refrigeration and hot water heating/steam production. Adding to this, higher efficiency, lower price and the sustainable solution that offering CO2 in general over HFC refrigerants, advocates this technology as a good candidate to be implemented inside cooling systems. [50,52–54].

The basic layout of TC CO2 HP is composed of an evaporator, a high-pressure compressor, a gas cooler, an internal heat exchanger, and an expansion valve.

As shown in Fig. 3, the main difference between a typical heat pump and *trans*-critical heat pump is the refrigerant in the upstream process does not undergo the phase change and remains in gaseous state. As a result of this intervention, less work is needed for compression process since the heat transfer process is taken place only though sensible load. One of the distinct differences between *trans*-critical cycle and sub-critical one is the pressure ratio between up and down stream flow. In trans- critical cycle such value is much higher. CO_2 critical point dictates the upper pressure always greater than 75 bar which would be recommended to be in the range of 100–140 bar for better performance. The increase of pressure ratio rises the thermodynamic losses during expansion [49]. To address this drawback, as shown in Fig. 4, an internal heat exchanger is set to recover discharged heat of the gas cooler avoiding the sharp transition that takes place inside the expansion valve. Such heat instead, could still be used to increase the temperature of the low-pressure refrigerant flowing into compressor. In this way, thermodynamic properties of the refrigerant before expansion process are smoother than before and useful heat will be redirected. Such heat pump system has the coefficient of performance in range of 3.0 and usually is able to produce hot water up to 90 °C [33].

Methodology

Case study and energy model

The city of Rome in Italy is considered as the reference location for meteorological data in these simulations (Table 1). An office building inside the city with the floor surface of 2489 m^2 is the case study which is implemented inside the REVIT environment. The temperature and absolute humidity profile of Rome in 2016, are brought in Fig. 5, respectively. Fig. 6 also provides a 3-D model of the building. In total, 100 air conditioning spaces are defined for the building, which are classified into four different usages: office, restroom, lobbies, and corridors. Such division inside REVIT facilitates sensible and latent heat calculation based on the type of activity and estimation of the number of people per unit of floor surface. According to the literature [56], the average adult, seated and working, generates excess heat at the rate of approximately 132 W. About 60% of this heat is transferred to the surrounding environment by convection and radiation, and 40% is released by perspiration and respiration.

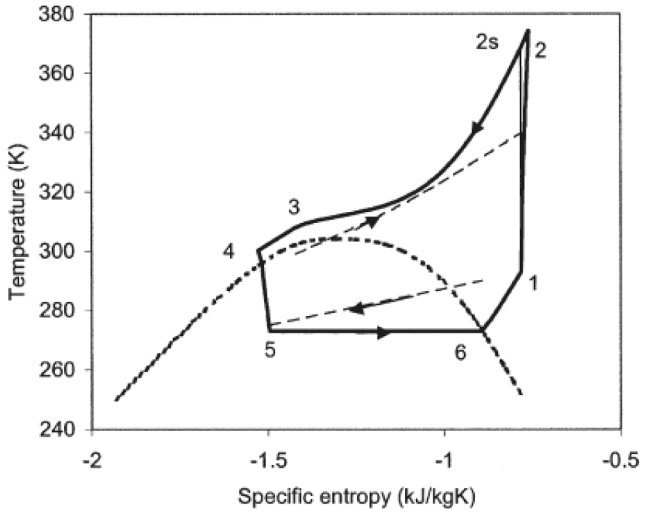

Fig. 3. TC CO2 HP T-s Diagram [55].

In the next step, dynamic heating and cooling load calculation are carried out to satisfy the comfort zone for the building as a unit in every interval. Based on ASHRAE standards in the building sector, in summer the threshold temperature for cooling is set to 26 ℃ and in winter, for heating, the temperature is set to 20 ℃. The relative humidity is always kept below 50%. Another parametric design to account for is the cross section of ducts for the airflow which has been carried out to meet the minimum air supply in accordance with the Italian technical standards [UNI 10399]. In accordance with the mentioned standard, the minimum air supply for a zone can be carried out from the Eq. (1):

$$f_{air} = Pe \times N \tag{1}$$

Where f_{air} is the minimum flow rate of the air.

Pe is the average number of people that occupy the zone.

N is the specific flow rate that is determined based on the type of activity that takes place in that zone (m^3/s/person). Such a value is obtained from the reference table available that is assigned to each zone based on the type of activity.

The total air flow rate can be simply calculated from the sum of all zona's minimum airflow:

$$f_{total} = \sum_{i=1}^{n} f_i \tag{2}$$

The total airflow rate for the building is 9990 l/s. The size of the duct can be derived considering the air velocity and the required flowrate:

$$v_{air} = W.H.f_{air} \tag{3}$$

Where W and H are the width and height of the duct respectively.

For the public building, the velocity of the air intake from the outside is in the range of 2.5 to 4.5 m/s [57]. Assuming 3 m/s for the velocity and square cross-section duct (W = H):

As can be seen from Table 2, assuming only one or two ducts require a very big duct cross-section As a result, at least three air handling units are assumed for the air supply since the cross-section would be reasonable in this case.

To create the building energy model, more consideration regarding standards in the building sector are needed to be assigned. According to the Italian regulation [58] which indicates U-values of each cavity and glazing needed to be provided, the material and insulation of the building is determined. Consequently, the dynamic load calculation over one year period has been performed. The simulation in this phase is carried out by software Career HAP (Hourly Analysis Power). Fig. 7 summarizes the simulation outcomes categorized into summer and winter hourly profiles.

Scenarios description

In this paper a hybrid solar cooling system based on desiccant wheel is simulated. As explained earlier, desiccant wheel system requires thermal power for regenerating the return air flow. The regeneration section is composed of TC CO_2 heat pump which could be integrated

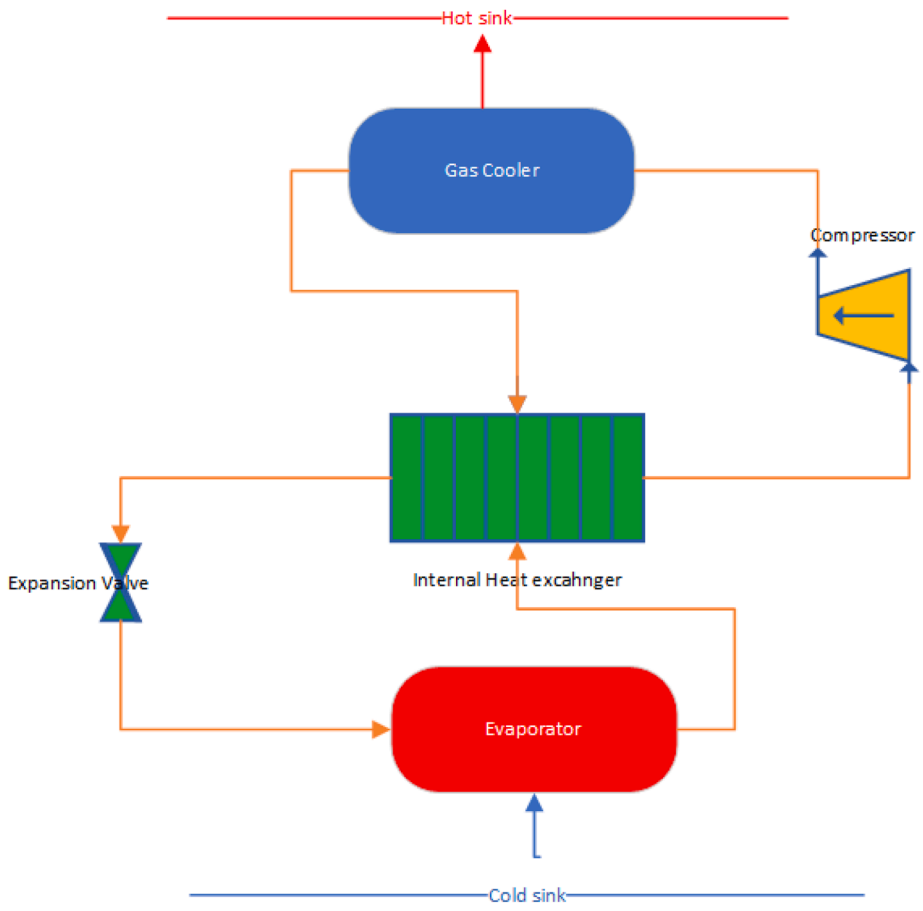

Fig. 4. Schematic diagram of TC CO_2 HP.

Table 1
Climate data of Rome.

Longitude	12 30 E
Altitude	24 *m*
Average Temperature winter	9℃
Average Temperature summer	22.5 ℃
Relative Humidity %	72
Average Horizontal solar radiation (W/m^2)	462

with solar thermal collectors and thermal storage system. As a result, four different configuration of TC CO2 heat pump integrated with DW have been proposed as follows. Fig. 8 shows the general configurations related to all cases together. The description of each scenario is specified in the following sub sections.

In Fig. 8, the mainstream air is always imported from the point 1. In both sub-layouts of Scenario 2, the mainstream air undergoes a pre-cooling process through cooling coils (CC). The working principle of the cooling effect is the same for all as introduced earlier in section 1.1. The main difference, however, is the contribution of TC CO_2 HP. The HP unit itself is consist of cold sink, and the hot sink along with the compressor, internal heat exchanger and expansion valve. In all configurations, the hot sink is used for regenerating the hot air for DW. In the other hand, the cold sink consists of cooling load required for mainstream air including also precooling coils (for sub-scenarios 2). In this case, the cold sink is formed by two sub-heat exchangers (evaporator).

Scenario 1

Fig. 8, a) reveals the schematic of Scenario 1. In this case, renewable share is characterized by both thermal collectors and photovoltaic. Solar thermal power is captured in a vessel. The heat pump contributes to the cooling process by capturing the heat from input airflow (point 3) and store it in the vessel. Along with HP, thermal collectors contribute to vessel thermal input. Such a thermal power must be sufficient to provide hot water at 90 °C to deploy in regeneration air flow at 65 °C. An electric heater is considered as a backup for vessels. That layout previously is accomplished and discussed in [33]. Huge rooftop space demand and installation along with relatively complex figures demerit Scenario 1. However, it features high renewable share. Moreover, the use of a storage tank guarantees the temperature threshold for the regeneration sector. As mentioned also in [59], the performance of desiccant material is drastically influenced by temperature in the regeneration sector.

Scenario 2; close loop

Scenario 2 is proposed in a relatively simpler layout with less equipment to save more rooftop space and consequently become more economically friendly. The heat transfer process inside the gas cooler takes place directly from CO2 to air. Such intervention allows to eliminate storage tank from the system as well as solar collectors which enable more available roof surface for PV installation. HP is exclusively corresponding the heat load of regeneration sector. As a result, the size of HP unit in this case must be increased. One practical solution is to increase the cooling load of evaporator. As illustrated also in Fig. 10c, the evaporator is consisting of two separate parts. The first evaporator corresponds to the pre-cooling process before the entrance into DW. The second one however is the regular cooling coil before supplying the air to the indoor ambient. To operate both evaporators simultaneously, the output temperature is fixed to 26 °C. In this way, fluids become reunified again after phase change process in both heat exchangers through a mixing valve.

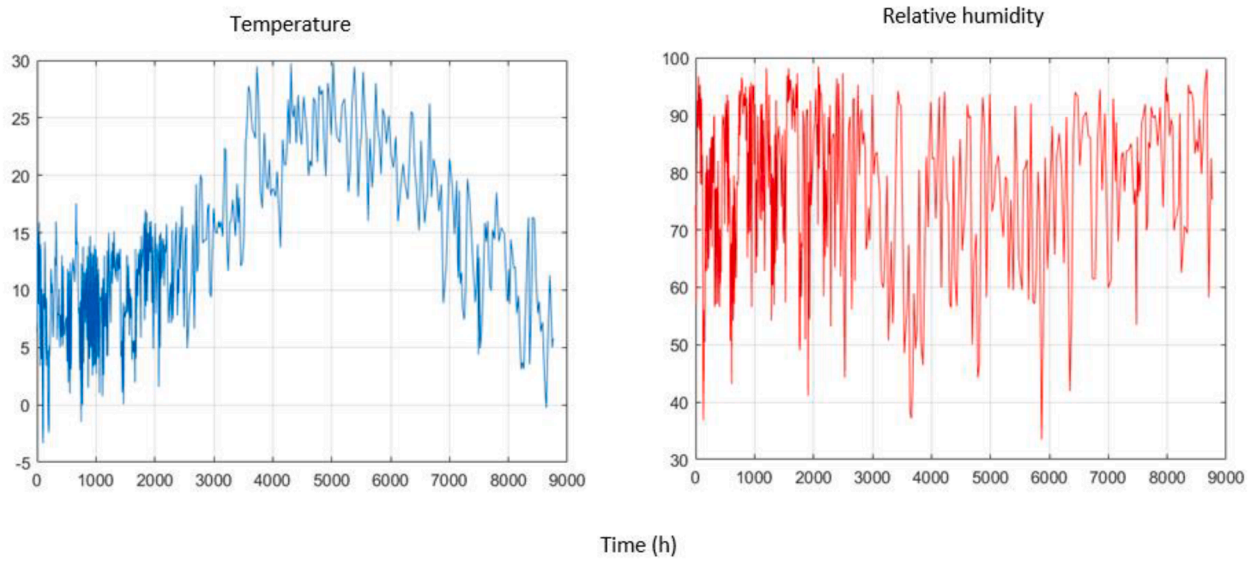

Fig. 5. Temperature and relative humidity data of city of Rome.

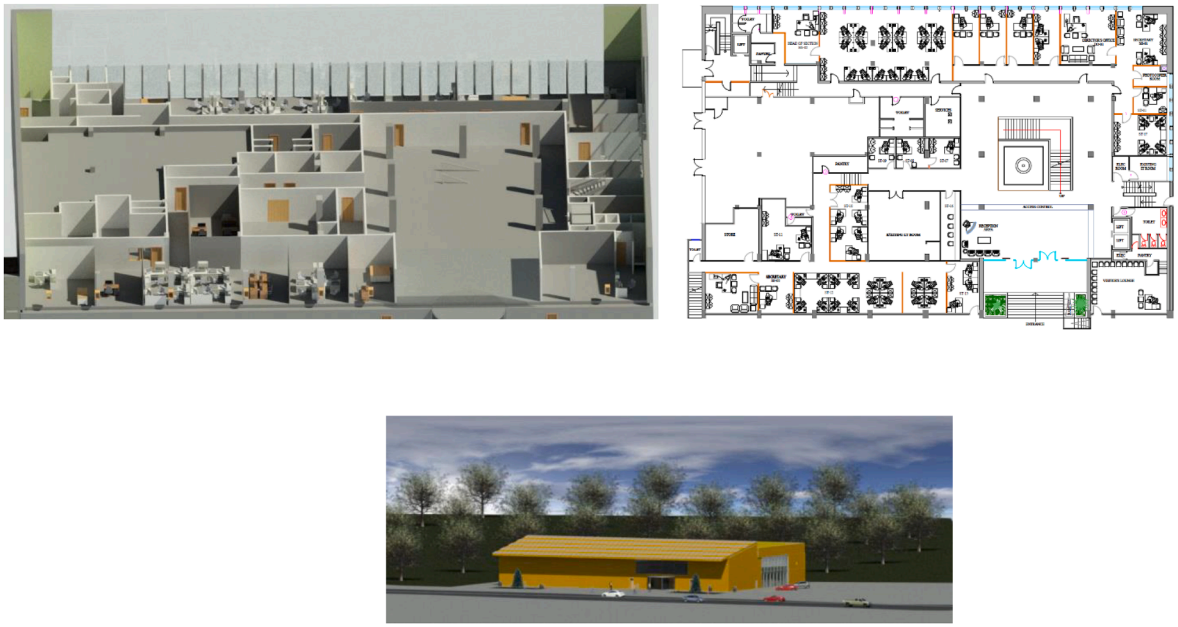

Fig. 6. A,b,c. 2_d and 3_d view of the case study office building.

Table 2
AHU duct size.

N duct	v(m/s)	airflow(m3/s)	W*H	W	H
1	3	9.99	3.33	1.82	1.82
2	3	5.00	1.67	1.29	1.29
3	3	3.33	1.11	1.05	1.05
4	3	2.50	0.83	0.91	0.91
5	3	2.00	0.67	0.82	0.82

Scenario 2; open loop

The open loop the is proposed with slight difference previous scenario. As explained in Fig. 8b, the return air is replaced with the fresh air as an input of heat pump. Like the former sub-Scenario 2, two evaporator units are implemented and work in the same way as explained before. Importing fresh air for return cycle requires some modification in mathematical model. Since the mass flow rate of fresh air used in the HP is not necessarily the same as previous, the new mass flow rate should be calculated. To optimize the mass ratio between process and returned air, the process air P_{in} and exhaust air R_{out} should satisfy the following equation, as reported in literature [42].

In Fig. 9, P_{in} is the process air inlet, P_{out} is the process air outlet, R_{in} indicates the regeneration air inlet and R_{out} the regeneration air outlet.

$$\frac{x_{Rin} - x_{Rout}}{x_{Pout} - x_{Pin}} = \frac{h_{Rout} - h_{Rin}}{h_{Pin} - h_{Pout}} \tag{4}$$

Such a point on the psychometric chart is considered as the optimum design point in which inlet and exhaust lines are parallel as shown in Fig. 11. In case of insufficient regeneration air supply, the wheel is unable to adsorb enough humidity from the process air flow (i.e. $RH_{Pout} < RH_{Pout\_desired}$).

Conversely, if regeneration air flow is higher than the designed value, though the process air desired condition would be satisfied, the wheel is unable to extract all the humidity that captured in the first

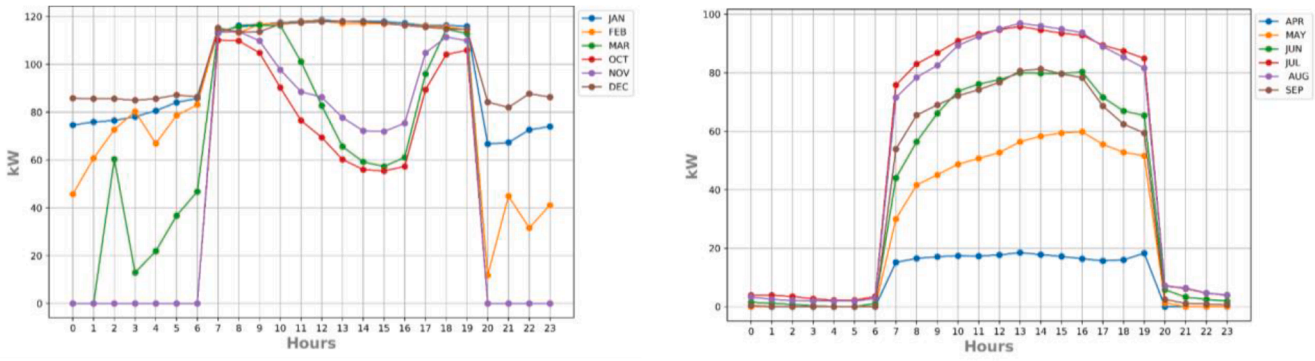

Fig. 7. Simulations results over 24 h by months: a) Cooling load profiles. b) Heating load profiles.

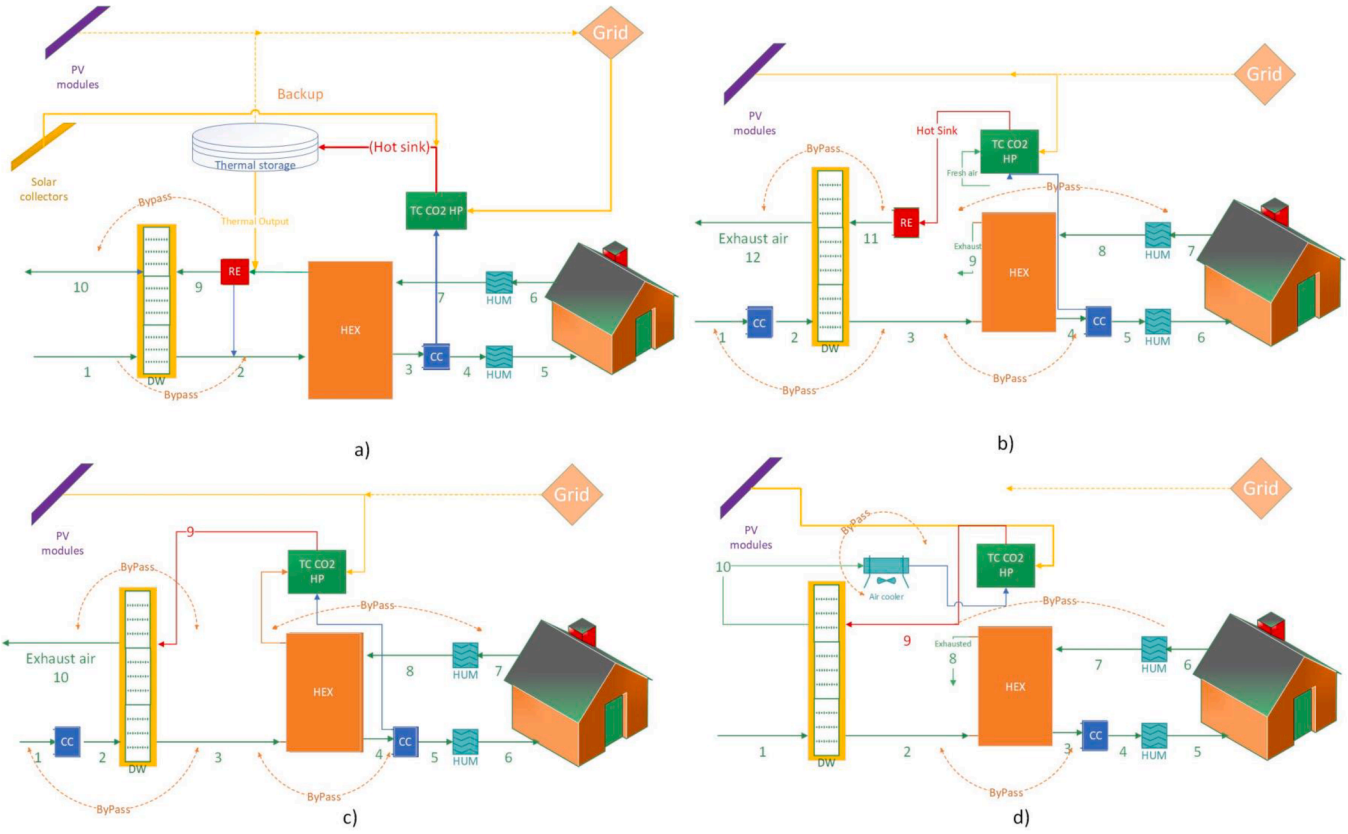

Fig. 8. Schematic of all scenarios: a) Scenario 1; b) Scenario 2 open loop; c) Scenario 2 close loop; d) Scenario 3Figure 8 Schematic of all scenarios: a) Scenario 1; b) Scenario 2 open loop; c) Scenario 2 close loop; d) Scenario.

place.

(Namely, $RH_{Rout} < RH_{Rout\_desired}$).

Scenario 3

A new potential contribution of TC CO2 heat pumps inside DEC unit is proposed in Scenario 3 [60]. As shown in Fig. 8d, the TC CO2 heat pump will be used exclusively in a close loop regeneration sector of the DEC unit. Hence, the exhaust air flow (R_{out}) that in previous scenarios discharges to the ambient, is employed to form a close loop cycle. Such an airflow is characterized by high temperature and high humidity ratio.

Starting from DW exhaust (R_{out}), the air flow is cooled down by the ambient air through a heat exchanger. The cooled air stream flows through the HP and undergoes the heating process to be regenerated. The regeneration air is exported again back to the DW.

Simulation

In this section the main correlations and assumptions regarding the main components modelling of the system are explained. The air stream in each point and after any intervention, is described by a set of thermodynamic and ambient properties including enthalpy, temperature, relative and absolute humidity as well as the mas flow rate (i.e., *h, T, RH, X, m,* respectively). The impact of each component has been evaluated by altering one or several mentioned properties. The input air stream is characterized with T_{amb} and RH_{amb} which are obtained from climate data. Additionally, $\dot{m}_{air}$ value has been fixed previously in section 2.2. The return air flow in the other hand, is set 26 °C and *RH* equal to 50%. Furthermore, T_{regen} *is set to 65 °C.* For solar radiation input, satellite data from PV GIS [61] have been imported and post processed for creating the timeseries. The final energy balance of all systems is shown in

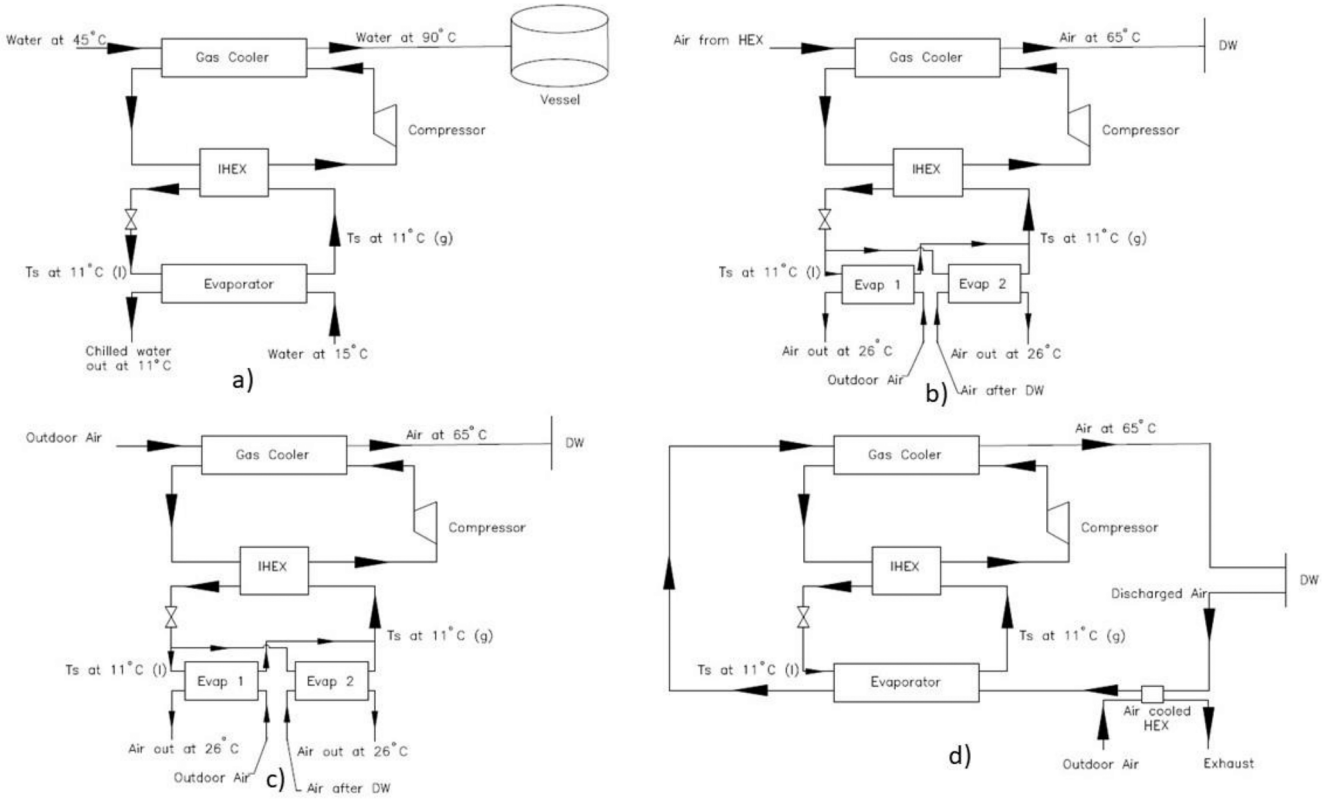

Fig. 10. Energy balance of cooling system, a) Scenario 1, b) Scenario 2 open loop, c) Scenario 2 close loop, d) Scenario 3.

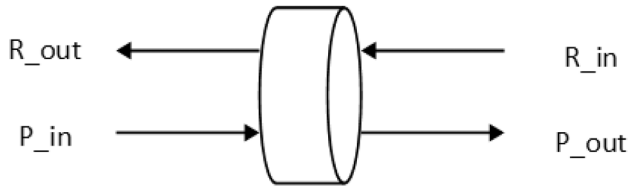

Fig. 9. DEC ports.

Fig. 10.

DW

The desiccant wheel model is created based on the experimental correlation for Silica Gel Type 1 found in the literature according to the work of Beccali et al. [46]. Such a model determines *h* and *RH* of wheel's output as follows:

$$h_{out} = 0.1321h_{regen} + 0.8688h_{in} \tag{5}$$

$$RH_{out} = 0.9428RH_{regen} + 0.0572RH_{in} \tag{6}$$

Consequently, T_{out} and X_{out}, can be calculated for the wheel. From Eq. (6) it is possible to calculate the total absolute humidity removal by the wheel from the main air stream, as reported in Eq. (7).

$$\Delta X_{wheel} = X_{in} - X_{out} \tag{7}$$

The bypass control system is designed to skip intervention when it is not necessary. Basically, when T and RH of the mainstream are below the set points values, the system operates in free cooling mode. Those conditions for both heat exchanger and desiccant wheel can be summarized as follows:

$$\begin{cases} if \quad T_{amb} \leqslant 26\ ^{\circ}C; & HEX\ bypass\ ON; \\ if \quad RH_{amb} \leqslant 50\%; & DW\ bypass\ ON \end{cases} \tag{8}$$

TC CO_2 HP

The heat pump is sized differently in each scenario. Indeed, in Scenario 1, the main refrigerant is water. The required mass flow rate of CO_2 is calculated to produce hot water at a constant temperature (90 °C). As a result, the energy balance of the gas cooler can be written as follows:

$$Q_{gas\ cooler} = \dot{m}_{water}(h_{hot_{water}} - h_{cold_{water}}) = \dot{m}_{CO2}(h_{CO2_{up\ pressure}} - h_{CO2_{down_{pressure}}}) \tag{9}$$

$$W_{compressor} = \frac{\dot{m}_{CO2}\,\Delta h_{iso}}{\eta_{iso}} \tag{10}$$

$$Q_{evap} = Q_{gas\ cooler} - W_{compressor} \tag{11}$$

Where,

Δh_{iso} represents the isentropic enthalpy increase that happens inside the compressor and η_{iso} is isentropic efficiency which is set to 0.78. The saturation condition of CO_2, in terms of temperature and pressure, is fixed to 11 °C and 46.6 bar, respectively.

Q_{regen} in this case, is the total amount of thermal energy received from HP and the solar collectors which the vessel stores:

$$Q_{regen} = Q_{vessel} = Q_{solar\_collector} + Q_{hot\_HP} + Q_{backup} \tag{12}$$

For all the other scenarios, excluding water, the heat transfer takes place directly between CO_2 and the air. Hence, Q_{regen} should be entirely provided by HP:

$$Q_{regen} = Q_{hot\_HP} + Q_{backup} \tag{13}$$

The backup system is always accounted for to ensure the continuous operation.

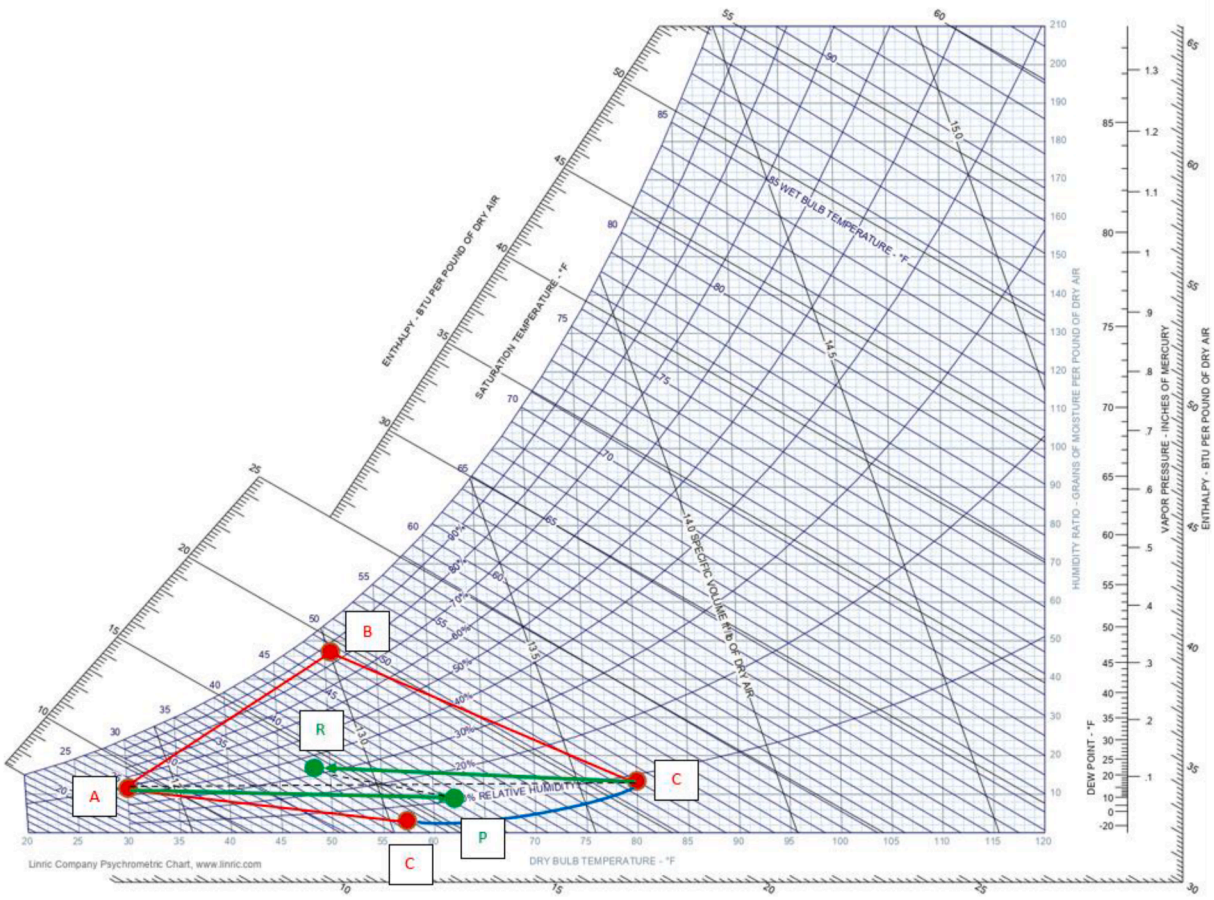

Fig. 11. Psychometric condition of closed regeneration loop; A: process inlet, C: regeneration inlet, P process air after passing wheel, R: regeneration exhaust, B and D constant relative humidity curve line. Psychometric chart from: https://www.engineeringtoolbox.com.

Multicriteria analysis

In order to indicate all of scenarios' performance and to compare each other in a systematic way, multicriteria analysis is carried out based on energy, economic and environmental indicators. In this section, those indicators are introduced, and the final outcomes have been reported in the Result and Discussion part.

Economic index

The Economic Index (I_{ECO}) can be decomposed into three elements: The mean actualized cash flows over the investment economic horizon (i.e I_{FC} weighted by x_1), the initial investment (i.e., I_{INV} weighted by x_2) and the Discounted Payback Period (i.e., I_{PBP} weighted by x_3):

$$I_{ECO} = I_{FC} + I_{INV} + I_{PBP} \tag{14}$$

where I_{FC} is the cash flow index and derived from:

$$I_{FC} = x_1 FC_i / FC_{max} \tag{15}$$

Here, FC_i is the mean cash flow calculated over the system lifetime associated to the specific *i-th* scenario, and FC_{max} is the maximum value among the mean cash flows related the all technical options which have been addressed.

Using the same approach, it is possible to define the remaining indicators:

$$I_{INV} = x_2 INV_{min} / INV_i \tag{16}$$

Where INV_{min} is the minimum investment (expressed by euro) among all the considered scenarios and INV_i is the one related to the specific option.

Finally,

$$I_{PBP} = x_3 PBP_{min} / PBP_i \tag{17}$$

Where PBP_{min} is the minimum PBP among all of the scenarios and PBP_i is the one for the *i-th* solution. For calculations, x_1, x_2, x_3 are assumed equal to 0.3, 0.4, 0.3, respectively.

The investment assumptions have been made based on what was found in literature and also on the market prices available on the benchmark. [62,63]. The CAPEX values related to each technical option have been outlined in Tables 3–5 respectively. Table 6 summerizes the economic indicators of each scenario.

Energy index

The energy index is related to the primary energy saving for each layout respect to maximum saved primary energy:

$$I_{EN} = PE_i / PE_{max} \tag{18}$$

Another helpful energy indicator is the renewable energy share

Table 3
CAPEX Scenario 1.

Scenario 1	
Component	**Capital cost**
DEC system	€ 160,704.00
Heat Pump	€ 26,755
Solar collectors	€ 31,248.00
Vessel	€ 54,000.00
PV_modules	€ 390,000.00
SUM	**€ 708,658.73**

Table 4
CAPEX Scenario 2.

Scenario 2	
Component	**Capital cost**
DEC system	€ 160,704.00
Heat Pump	€ 25,460
PV_modules	€ 546,000.00
SUM	**€ 732,164**

Table 5
CAPEX scenario 3.

Scenario 3	
Component	**Capital cost**
DEC system	€ 160,704.00
Heat Pump (x2)	€ 50,921.00
PV_modules	€ 546,000.00
SUM	**€ 757,625.00**

Table 6
Summary of economic of indicators.

Scenario	i	NPV	IRR	PBP	Lifetime [64–66]
1	3%	€ 532,307.53	10%	9	20
2 close loop	3%	€ 664,750.62	11%	7	20
2 open loop	3%	€ 773,070.54	13%	8	20
3	3%	€ 766,855.26	16%	7	20

(RES) of each configuration, which can be divided into electric and thermal contribution:

$$RES_{elec} = \frac{E_{renewable}}{E_{total}} \tag{19}$$

$$RES_{th} = \frac{Q_{renewable}}{Q_{total}} \tag{20}$$

The RES_{ele} is the energy received from PV modules, whilst the RES_{th} consists of the solar thermal collectors' contribution (only in the first scenario) and the heat discharges from the TC CO_2 HP.

To evaluate the HP performance, to provide heat and cooling effect, two correlations are presented. The coefficient of performance (COP) is used to describe the HP heat performance [67]. Such a number can be derived from Carnot ideal cycle and also the actual value as follows:

$$COP_{HP\_actual} = \mu \bullet COP_{HP_{Carnot}} = \mu \bullet \left(\frac{T_{cond}}{T_{cond} - T_{ev}}\right) \tag{21}$$

In Eq. (21), μ is the thermodynamic perfection factor which has the value in the range 0.4–0.6 [33]. Notwithstanding, the actual COP once the real data are available, can be also calculated by using the common definition of performance as reported in literature [68]:

$$COP_{actual} = \frac{Q_{Gascooler}}{W_{compressor}} \tag{22}$$

For evaluating the cooling effect caused by the HP, energy efficiency ratio (EER) is used which take into account the amount of heat captured by the evaporator:

$$\text{EER} = \frac{Q_{Evaporator}}{W_{compressor}} \tag{23}$$

The total COP of the cooling system can be evaluated considering the electric and thermal energy consumed to provide cooling effect. In this way, the COP_{elec} and COP_{th} are introduced:

$$\text{COP}_{\text{elec}} = \frac{P_{cooling}}{P_{elec}} \tag{24}$$

In Eq. (24), $P_{cooling}$ basically is the cooling load of the envelope and P_{elec} is the electric consumption excluding renewable generation.

$$\text{COP}_{\text{th}} = \frac{P_{cooling}}{P_{regen}} \tag{25}$$

In Eq. (25), P_{regen} is thermal energy imported from an external resource for return air regeneration.

Environmental index

Environmental index is a function of the reduced CO_2 emissions on the environment, expressed in terms of tons per year, for each intervention respect to the maximum reduction among all interventions. Thus, it reads as follows:

$$I_{ENV} = CO_{2i}/CO_{2max} \tag{26}$$

Results and discussion

Performance of the TC CO_2 heat pump

In accordance with the temperature values assumed for simulating the hybrid system, the ideal Carnot COP of the HP has been calculated and it is depicted in Fig. 12. As suggested by results, in the ideal Carnot cycle, Scenario 3 offers a significant improvement among all. Such a behaviour is due to the heat sinks temperature levels difference between the evaporator and gas cooler. The gas cooler (hot sink) in all scenarios provides the required regeneration power to heat up the air at 65 °C before it passes through the DW. The actual COP results are reported in Fig. 13. In Scenario 3, the cold sink temperature is formed by the exhaust air of DW. That stream featuring high amount of water content and high temperature, is cooled down by fresh air and after it is used in the evaporator loop. Moreover, the same air stream is delivered to the gas cooler section. Eventually, the ΔT between HP cold and hot sinks, significantly decreases, it boosts up the COP. It is noteworthy that the simulation is carried out for the same down and upstream pressure in each scenario.

There is also a slight difference between Sub Scenarios 2 due to the cycle configurations. By, the use of fresh air in the return process, it is possible to get to the better performance. Such a result was expected since in a major part of the summer period the ambient temperature is generally higher than 23 °C, which is basically the gas cooler inlet temperature. As a result, the temperature drop inside the gas cooler is lower than the close loop configuration and less compression work is needed in this layout.

Renewable energy share

The renewable share of Scenario 1 includes the contribution of both solar collectors and solar PV modules. In detail, PV array electricity production corresponds to nearly half of the building electric load, including equipment, lights, auxiliaries, and HP itself. In two Sub-Scenario 2 however, the effect associated to the vessel and solar collectors' removal, disposes more available rooftop space to increase PV module installation. Therefore, the RES_{elec} increases in these two Sub-Scenarios. Between those ones, the open loop is characterised by a smaller compressor work leading to a slight decrease in the electric consumption. Likewise, the significant improvement is offered by Scenario 3, where the HP can provide 100% of the thermal load for regenerating the DW. This is due to the huge amount of thermal energy that could be discharged by HP, which is 6.5 times higher than the electric consumption of such device. The simulation outcomes have been summarized in Fig. 14.

Environmental impact

The effect of seasonal climate parameters variation on the HP

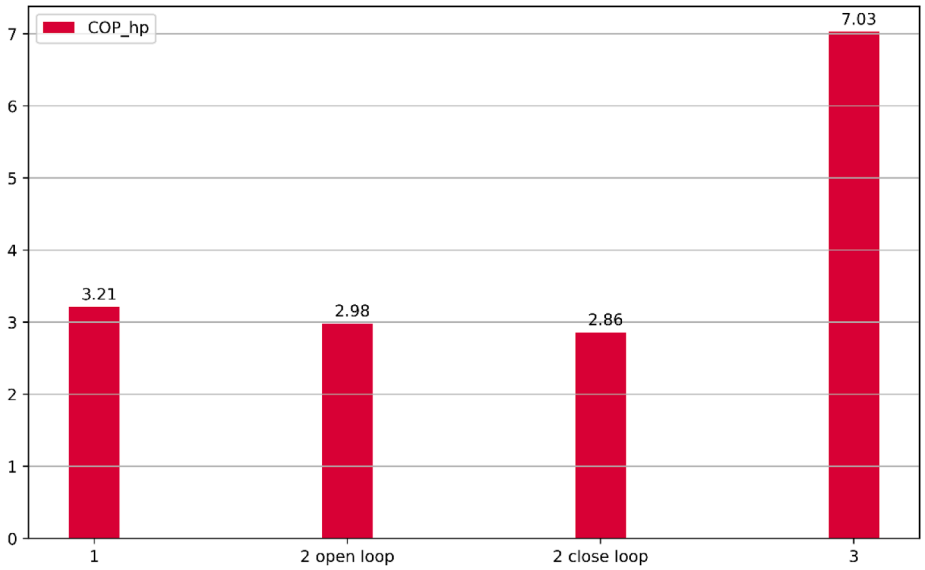

Fig. 12. Heat pump Carnot ideal COP.

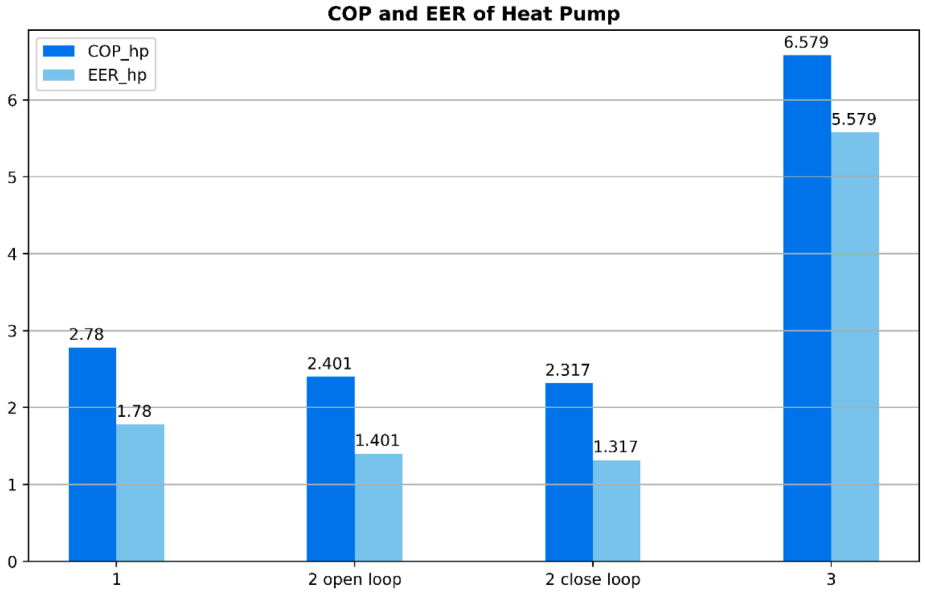

Fig. 13. COP and EER of HP.

performance in each scenario is different. As shown in Fig. 15, the efficiency fluctuations of Scenario 1 are minimal. This is due to the presence of the vessel that ensures constant thermal power required for regeneration, despite the variation of cooling load. Therefore, the COP in this system is weakly dependent on climate variations.

Scenario 2 close loop has a constant thermal load to the gas cooler. This is because of the constant inlet temperature the return air which is kept at 23 °C. Conversely, the cooling load hourly changes according to the outdoor environmental temperature variations. From data it emerges how, in July and August, where temperatures are maximum, the COP accomplishes the highest value. Therefore, it is possible to state that such a system has better performance when the outdoor temperature is the highest.

However, in Sub-Scenario 2, namely the open loop, the climate variations affect the thermal load at gas cooler side as well as the cooling load to the evaporator. As suggested by results, during months of July and August whereas the maximum temperatures are recorded, the provided heat is minimal and the COP decreases. In the other words, the outdoor environmental conditions have more impact on the cooling load (Q_c) than heat load (Q_h). To improve COP in such a system, the regeneration temperature should be increased more starting from 65 °C. In so doing, the effect of cooling load raise can be taken under control.

In Scenario 3 another phenomenon influences the HP performance, which needs additional consideration. Since in this case the TC CO_2 heat pump forms a close loop with the regeneration section for the DW. The exhaust air is characterized by a significant water content that is now redirected towards the gas cooler. The heat exchange with fresh air in the air cooler can decrease the outlet temperature up to values lower than the dew point. Therefore, the huge humidity content tends to condense out in the air stream and it must be drained before regenerating again the wheel. According to the simulations, during the summertime, in a city such as Rome characterized by a moderately high humidity profile, to avoid droplets formation the regeneration temperature must be increased from 65 °C to at least 95 °C. In this case, to avoid COP drops, the cold sink temperature should also be modified from 11 °C to 25 °C.

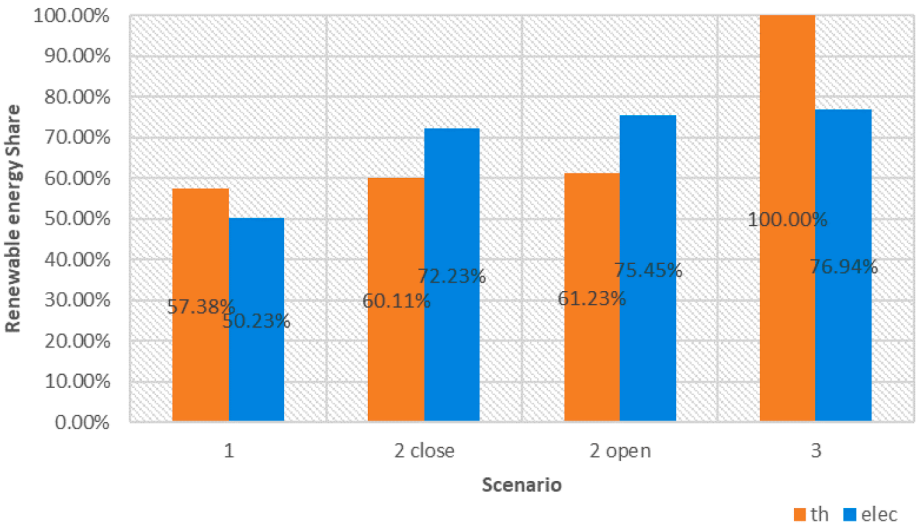

Fig. 14. Renewable energy Share.

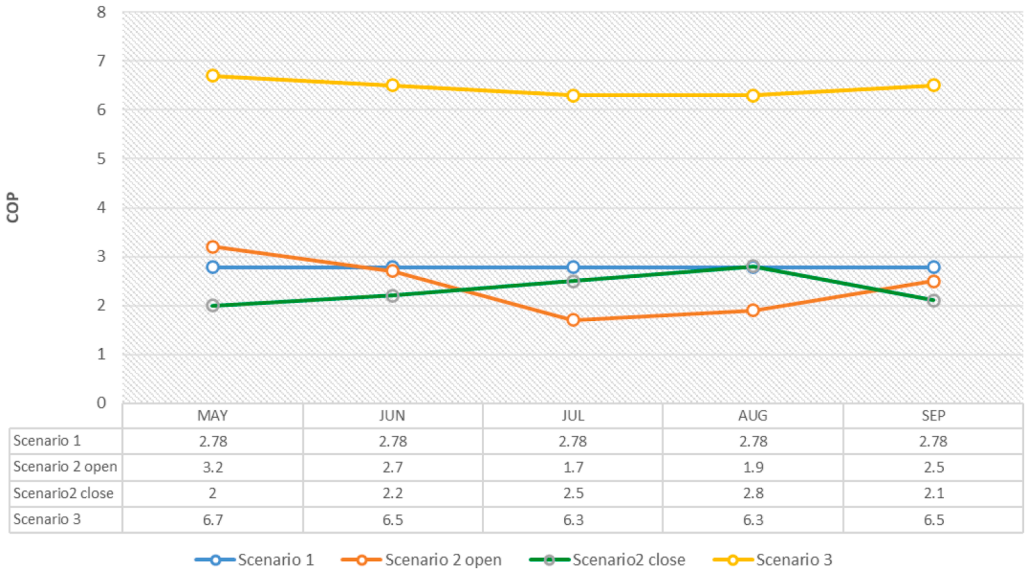

	MAY	JUN	JUL	AUG	SEP
Scenario 1	2.78	2.78	2.78	2.78	2.78
Scenario 2 open	3.2	2.7	1.7	1.9	2.5
Scenario2 close	2	2.2	2.5	2.8	2.1
Scenario 3	6.7	6.5	6.3	6.3	6.5

Fig. 15. COP of the HP over summer period.

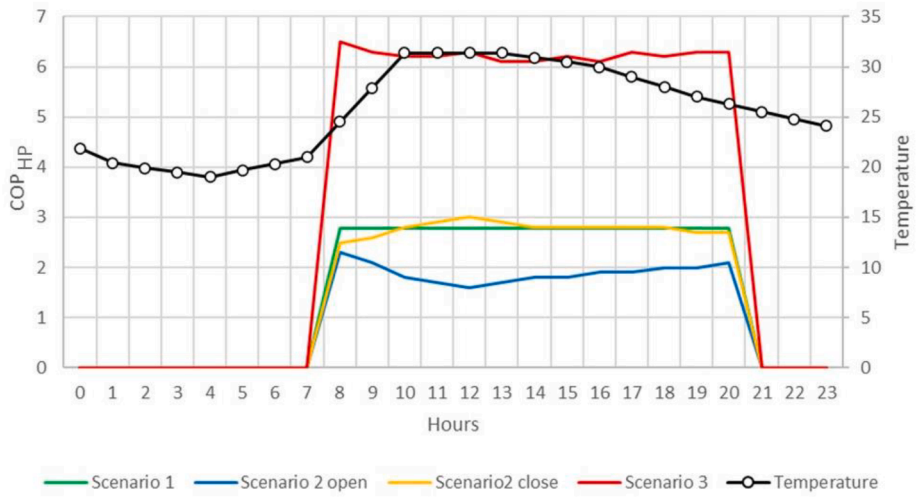

Fig. 16. A typical operation day in July.

Fig. 16 reveals the HP system performance in a typical summer day. The environmental data for calculations refer to the 15th of July. As the temperature increases during the daylight the performance of Scenario 2 close loop tends to improve while the effect on the open loop is reverse. Scenario 3 does not really demonstrate a strict correlation with temperature, instead the absolute humidity is the most relevant parameter affecting the performance. Recalling the configuration in Fig. 10d, the airstream forms a close loop all over the cycle. The only interaction between outdoor air mainstream is the air-cooled heat exchanger in which only the sensible heat can be exchanged. As mentioned before, such an effect is minimal on the performance of the HP. However, the outdoor absolute humidity trend determines DW performance in terms of amount of captured water content inside the wheel. This is the starting point of the close loop regeneration cycle of Scenario 3. As absolute humidity increases, the captured water content inside the wheel accumulates. Such a phenomenon increases the possibility of the formation of water droplets inside the cycle and defects the energy performance of the HP.

Air handling unit recovery heat exchanger effectiveness

During the simulation period, a heat recovery exchanger is modelled assuming a constant heat transfer effectiveness. To improve the AHU energy performance, the impact of that parameter on the energy, economic and environmental indicators, has been investigated. Indeed, by changing the effectiveness value it is possible to notice different behaviours depending on the layout.

In Scenario 1, increasing heat transfer effectiveness (ε) results in discharging a higher heat transfer rate. Consequently, the outlet temperature to the cold side will be higher than before, while the hot side one shrinks. That issue has a positive effect since the airstream must be heated up at 65 °C by a reduced power to regenerate the DW On the other hand, the hot side of the heat exchanger, which determines the cooling load requirement, will be decreased since the outlet temperature in this stream is lower than before.

In Scenario 2 close loop, improving the effectiveness will lead to an increase in the outlet temperature of air stream inside the cold side (returned from the indoor environment) and decrease the temperature in the hot side, which eventually shrinks the cooling load of the secondary coils. Yet, on the cold side, increasing the temperature, is advantageous from the energy point of view, since the air stream flows through the TC CO_2 heat pump with higher temperatures. As a result, the temperature difference between hot and cold sinks will be shortened leading to higher COP values.

Nevertheless, in Scenario 2 open-loop and Scenario 3, the impact of effectiveness is different. In these two cases the air stream extracted from the building passes through the heat exchanger and then it is vented out. Consequently, the effectiveness increase affects only the outlet temperature of the main air stream contributing to reduce the required cooling load. Therefore, in Scenario 2-open loop the cooling coil size will be lower. Similarly, it occurs in Scenario 3 but in this case the additional HP unit has to be used for providing the cooling effect since the TC CO_2 is dedicated only to the regeneration process.

In Scenario 2 open loop, the heat pump cold sink is represented by the primary and secondary cooling coils. Notwithstanding, the heat exchanger effectiveness in these layouts influences only the secondary coil size. Indeed, as the effectiveness value increases the cooling load lowers and therefore the electricity consumption reduces as well.

Referring to Scenario 3, since the TC heat pump operation is only dedicated to the DW regeneration cycle, another typical heat pump will be employed to provide the building sensible cooling load. In this case, an inlet temperature reduction shrinks that energy amount served by the secondary heat pump, not affecting the size of the TC one.

Fig. 17 shows the footprint of heat exchanger effectiveness on all of the defined indexes. Generally speaking, the correlation of HEX effectiveness with all Scenarios except Scenario 3 has been realized linearly. In Scenario 3, $\varepsilon < 0.4$ results in a huge fall in all three energy, environmental and economic indexes. In the other words, in low

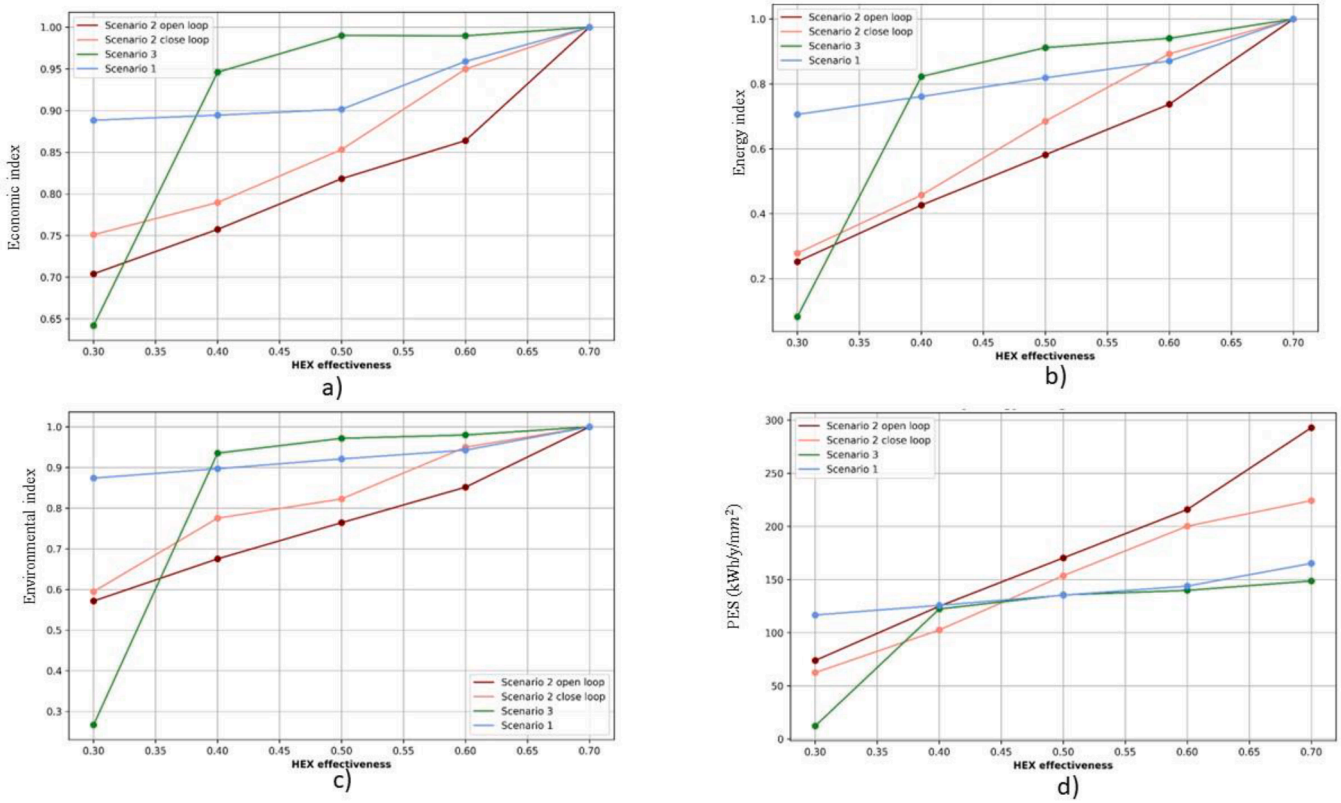

Fig. 17. The impact of ε on important indicators: a) Economic index; b) Energy index; c) Environmental index; d) Primary energy saving.

effectiveness region, Scenario 3 become the least interested case among all. Such a meaningful difference rises from disability of system to supply sufficient cooling effect for ε values below 0.4. Hence, the excess load should be provided through secondary heat pump system that increases the size as well as electric consumption. Such a trend in other Scenarios is not observed due to the absence of secondary heat pump unit. Comparing two sub-Scenarios 2, the close loop is preferred from energy, economic and environmental point of view. However, through Scenario 2 open loop, it is possible to save more primary energy sources. This is because of thermal load adjustment that applied in that Scenario to make it possible to reduce thermal consumption of the system. From the energy point of view, it is important to indicate how much primary energy can be saved in each case. Furthermore, the required receiving surface of renewable technologies is another crucial parameter to account for to properly assess the layout suitability. From Fig. 17d it emerges how, the Scenario 2 open loop represents the highest primary energy saving among all. It is worth mentioning that in both sub-Scenarios 2, the PV sizes are higher than in Scenario 3. Hence, logically the renewable energy generation rate for these two cases is larger than Scenario 3. In other words, Scenario 3 due to higher performance can provide the required heat with less roof surface comparing with Sub-Scenarios 2.

Air mass flow rate for regeneration

Referring to the open loop scenarios, the effect of regeneration mass flow rate on the performance of wheel's moisture removal has been investigated. In this section, two extreme cases, consisting of insufficient and overflow regeneration mass flow rates, have been simulated and discussed. According to [69], the mass flow rate increase would defect the COP of the whole cooling system. To analyse that issue an additional technical parameter has been defined. In detail, the MFRR (Mass Flow Rate Ratio), namely the ratio between the regeneration air mass flow rate and the process air mass flow rate, can be used and it reads as follows:

$$MFRR = \frac{\dot{m}_{reg,air}}{\dot{m}_{p,air}} \tag{27}$$

As a consequence, when the process mass flow rate is fixed, by increasing the MFRR values the system COP decreases. Thus, the higher the mass flow rate of regeneration air, improves the wheel humidity removal.

For instance, referring to the Scenario 3, the seasonal system COP vs MFRR has been superimposed to the moister removal capacity associated to the DW, as reported in Fig. 18.

Considering these two curves, their intersection identifies the optimal MFRR value, which represents a compromise between the highest achievable energy performance and the largest moisture removal by the DW. Indeed, by using regeneration mass flow rates higher than the optimal one, even though the System COP increases. Higher flow rate values from the optimal one result in higher moisture at the exposure of the wheel. On the other hand, declining from it disables DEC to provide a sufficient evaporative cooling process.

This behaviour can be observed by considering Fig. 18 describing the behaviour of Scenario 3, involving regeneration airflow rates different from process one. The intersection between two curves, determines the optimum point.

Consequently, the optimal mass flow rate ratio can be chosen to optimize moisture removal of the wheel.

Conclusion

This paper investigates the potential improvement of the energy performance of the DEC system to provide interior conditioned air. In so doing, a hybrid system composed of renewable sources (solar) DEC unit and TC CO_2 HP has been introduced and four different layouts are examined. The main outcomes of this work can be summarized as follows:

- The dynamic simulations over one year period showed through scenario 3 remarkable COP values are reachable for the TC CO_2 HP, namely up to 6.5.
- The results suggest a strong dependency between the TC CO_2 HP COP and temperature curve. The best performance has been obtained on weather conditions that are characterized by high-temperature and high humidity values.
- In open loop type Scenarios, during the intervals that either temperature is not high enough or the moisture value is too low, the system showed relatively poor performance. In the other hand, Scenario involving close loop and the one integrated with vessel are less affected by climate variations.
- Heat exchanger effectiveness is recognized as a useful parameter to decrease the cooling load. In average considering all four scenarios, by increasing ε from 0.3 to 0.7, the energy index can be increased up to 80%.
- The return air flow rate in open-loop scenarios can be controlled to reduce the heat requirement for the regeneration sector. Even though

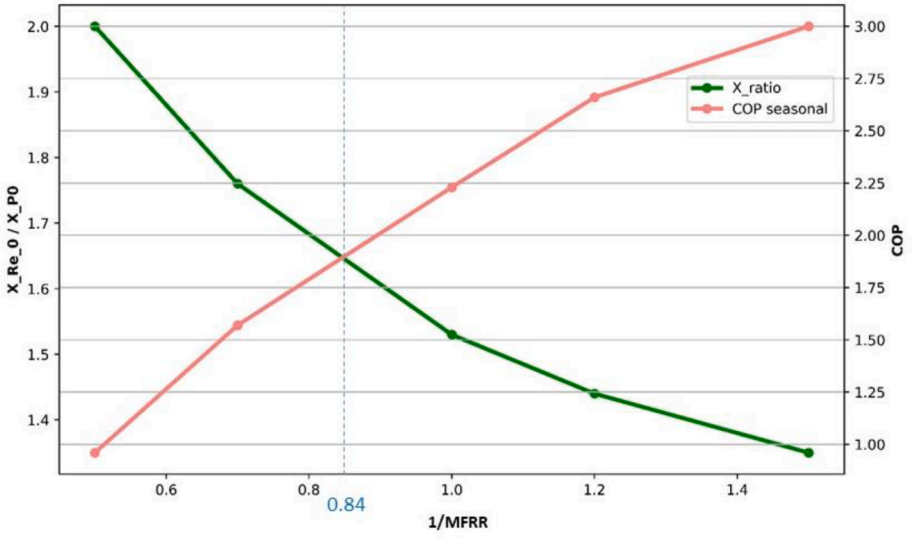

Fig. 18. Moisture removal capacity of the wheel and seasonal cop by changing mass flow rates of regeneration air, for scenario 3.

higher regeneration mass flow rates compromise heat pump COP, it also increases the wheel capacity of moisture removal. By confronting these two trends, the optimal regeneration mass flow rate for the system can be set. For Scenario 3 the mass flow ratio MFRR is obtained as $\frac{1}{0.84} = 1.19$.

In general, the performance of HP for heating purposes in summer is realized more efficient than cooling application. Since the COP is always higher than EER. Furthermore, in the summer the cooling load is the highest when the radiation has the peak value. Hence, more renewable power is available whenever more cooling load is required. The proposed cooling system has an acceptable performance in extreme climate conditions. However, the outdoor variation defects the performance in general. The future work can be defined with the scope of reducing as much as possible the cooling effect dependency to environmental fluctuation. 'The result of this work indicate a potential improvement on the performance of the desiccant-based cooling system in general and make it compatible with close loop benchmark technologies.'

CRediT authorship contribution statement

Gianluigi Lo Basso: Conceptualization, Methodology, Writing – review & editing. **Ali Mojtahed:** Data curation, Formal analysis, Writing – original draft. **Lorenzo Mario Pastore:** Writing – original draft, Software. **Livio De Santoli:** Supervision.

Declaration of Competing Interest

The authors declare that they have no known competing financial interests or personal relationships that could have appeared to influence the work reported in this paper.

Data availability

Data will be made available on request.

References

[1] No Title (n.d.). https://pris.iaea.org/PRIS/WorldStatistics.
[2] Kashif A, Ali M, Sheikh NA, Vukovic V, Shehryar M. Experimental analysis of a solar assisted desiccant-based space heating and humidification system for cold and dry climates. Appl Therm Eng 2020;175:115371.
[3] https://ec.europa.eu/energy/topics/energy-efficiency/energy-efficient-buildings/nearly-zero-energy-buildings_en, (n.d.).
[4] D'Agostino D, Zangheri P, Cuniberti B, Paci D, Bertoldi P, D'Agostino D, et al. Synthesis Report on the National Plans for Nearly Zero Energy Buildings (NZEBs) 2016. https://doi.org/10.2790/659611.
[5] Lo Basso G, Nastasi B, Salata F, Golasi I. Energy retrofitting of residential buildings—How to couple Combined Heat and Power (CHP) and Heat Pump (HP) for thermal management and off-design operation. Energ Build 2017;151:293–305. https://doi.org/10.1016/j.enbuild.2017.06.060.
[6] Lo Basso G, Rosa F, Astiaso Garcia D, Cumo F. Hybrid systems adoption for lowering historic buildings PFEC (primary fossil energy consumption) - A comparative energy analysis. Renew Energy 2018;117:414–33. https://doi.org/10.1016/j.renene.2017.10.099.
[7] L. De Santoli, G. Lo Basso, G. Spiridigliozzi, D.A. Garcia, Innovative hybrid energy systems for heading towards NZEB qualification for existing buildings. In: Proc. - 2018 IEEE Int. Conf. Environ. Electr. Eng. 2018 IEEE Ind. Commer. Power Syst. Eur. EEEI, (n.d.).
[8] Daou K, Wang RZ, Xia ZZ. Desiccant cooling air conditioning: A review. Renew Sustain Energy Rev 2006;10:55–77. https://doi.org/10.1016/j.rser.2004.09.010.
[9] Allouhi A, Kousksou T, Jamil A, Bruel P, Mourad Y, Zeraouli Y. Solar driven cooling systems: An updated review. Renew Sustain Energy Rev 2015;44:159–81. https://doi.org/10.1016/j.rser.2014.12.014.
[10] Kalogirou SA. Chapter3 – Solar Energy Collectors. Solar Energy Engineering. Second edition. Boston: Academic Press; 2014. p. 125–220., (n.d.).
[11] Zhiqiang Y. Development of solar thermal systems in China. Sol Energy Mater Sol Cells 2005;86:427–42. https://doi.org/10.1016/j.solmat.2004.07.012.
[12] Shirazi A, Taylor RA, Morrison GL, White SD. Solar-powered absorption chillers: A comprehensive and critical review. Energy Convers Manag 2018;171:59–81. https://doi.org/10.1016/j.enconman.2018.05.091.
[13] R. Narayanan, Heat-driven cooling technologies, Elsevier Inc., 2017. doi: 10.1016/B978-0-12-805423-9.00007-7.
[14] La D, Dai YJ, Li Y, Wang RZ, Ge TS. Technical development of rotary desiccant dehumidification and air conditioning: A review. Renew Sustain Energy Rev 2010;14:130–47. https://doi.org/10.1016/j.rser.2009.07.016.
[15] Camargo JR, Ebinuma CD, Silveira JL. Thermoeconomic analysis of an evaporative desiccant air conditioning system. Appl Therm Eng 2003;23:1537–49. https://doi.org/10.1016/S1359-4311(03)00105-4.
[16] El Hourani M, Ghali K, Ghaddar N. Effective desiccant dehumidification system with two-stage evaporative cooling for hot and humid climates. Energ Build 2014;68:329–38. https://doi.org/10.1016/j.enbuild.2013.09.040.
[17] Cejudo JM, Moreno R, Carrillo A. Physical and neural network models of a silica-gel desiccant wheel. Energ Build 2002;34:837–44. https://doi.org/10.1016/S0378-7788(02)00100-7.
[18] Zouaoui A, Zili-Ghedira L, Ben Nasrallah S. Open solid desiccant cooling air systems: A review and comparative study. Renew Sustain Energy Rev 2016;54:889–917. https://doi.org/10.1016/j.rser.2015.10.055.
[19] Çarpinlioglu MÖ, Yildirim M. A methodology for the performance evaluation of an experimental desiccant cooling system. Int Commun Heat Mass Transf 2005;32:1400–10. https://doi.org/10.1016/j.icheatmasstransfer.2005.07.008.
[20] Koronaki IP, Rogdakis E, Kakatsiou T. Thermodynamic analysis of an open cycle solid desiccant cooling system using Artificial Neural Network. Energy Convers Manag 2012;60:152–60. https://doi.org/10.1016/j.enconman.2012.01.022.
[21] Panaras G, Mathioulakis E, Belessiotis V. Solid desiccant air-conditioning systems - Design parameters. Energy 2011;36:2399–406. https://doi.org/10.1016/j.energy.2011.01.022.
[22] Hirunlabh J, Charoenwat R, Khedari J, Teekasap S. Feasibility study of desiccant air-conditioning system in Thailand. Build Environ 2007;42:572–7. https://doi.org/10.1016/j.buildenv.2005.09.022.
[23] Sheng Y, Zhang Y, Sun Y, Fang L, Nie J, Ma L. Experimental analysis and regression prediction of desiccant wheel behavior in high temperature heat pump and desiccant wheel air-conditioning system. Energ Build 2014;80:358–65. https://doi.org/10.1016/j.enbuild.2014.05.040.
[24] Tu R, Liu XH, Jiang Y. Performance analysis of a two-stage desiccant cooling system. Appl Energy 2014;113:1562–74. https://doi.org/10.1016/j.apenergy.2013.09.016.
[25] Gadalla M, Saghafifar M. Performance assessment and transient optimization of air precooling in multi-stage solid desiccant air conditioning systems. Energy Convers Manag 2016;119:187–202. https://doi.org/10.1016/j.enconman.2016.04.018.
[26] McNevin C, Harrison SJ. Multi-stage liquid-desiccant air-conditioner: Experimental performance and model development. Build Environ 2017;114:45–55. https://doi.org/10.1016/j.buildenv.2016.12.011.
[27] Baniyounes AM, Rasul MG, Khan MMK. Experimental assessment of a solar desiccant cooling system for an institutional building in subtropical Queensland, Australia. Energ Build 2013;62:78–86. https://doi.org/10.1016/j.enbuild.2013.02.062.
[28] Baniyounes AM, Liu G, Rasul MG, Khan MMK. Analysis of solar desiccant cooling system for an institutional building in subtropical Queensland, Australia. Renew Sustain Energy Rev 2012;16:6423–31. https://doi.org/10.1016/j.rser.2012.07.021.
[29] Ghali K. Energy savings potential of a hybrid desiccant dehumidification air conditioning system in Beirut. Energy Convers Manag 2008;49:3387–90. https://doi.org/10.1016/j.enconman.2008.04.014.
[30] La D, Dai Y, Li Y, Ge T, Wang R. Case study and theoretical analysis of a solar driven two-stage rotary desiccant cooling system assisted by vapor compression air-conditioning. Sol Energy 2011;85:2997–3009. https://doi.org/10.1016/j.solener.2011.08.039.
[31] R.F. de Oliveira, change the ChangetheRest, O. White, A.R. Kerlavage, R.A. Clayton, G.G. Sutton, R.D. Fleischmann, K.A. Ketchum, H.P. Klenk, S. Gill, B.A. Dougherty, K. Nelson, J. Quackenbush, L. Zhou, E.F. Kirkness, S. Peterson, B. Loftus, D. Richardson, R. Dodson, H.G. Khalak, A. Glodek, K. Mckenney, L.M. Fitzegerald, N. Lee, M.D. Adams, E.K. Hickey, D.E. Berg, J.D. Gocayne, T.R. Utterback, J.D. Peterson, J.M. Kelley, M.D. Cotton, J.M. Weidman, C. Fujii, C. Bowman, L. Watthey, E. Wallin, W.S. Hayes, M. Borodovsky, P.D. Karpk, H.O. Smith, C.M. Fraser, J.C. Venter, Enhanced Reader.pdf, Nature 388 (2018) 539–547.
[32] Bourdoukan P, Wurtz E, Joubert P. Experimental investigation of a solar desiccant cooling installation. Sol Energy 2009;83:2059–73. https://doi.org/10.1016/j.solener.2009.08.005.
[33] Lo Basso G, de Santoli L, Paiolo R, Losi C. The potential role of trans-critical CO2 heat pumps within a solar cooling system for building services: The hybridised system energy analysis by a dynamic simulation model. Renew Energy 2021;164:472–90. https://doi.org/10.1016/j.renene.2020.09.098.
[34] Whitaker S. Simultaneous heat mass and momentum transfer in porous media: a theory of drying, 13. Academic press; 1977. p. 119–203 (n.d.).
[35] Mhimid A, Ben Nasrallah S. Theoretical study of heat and mass transfers during drying of granular products. In: Turner I, Mujumder S, editors. Math- ematical modelling and numerical techniques in drying technology. New York: Marcel Dekker Inc; 1993381–41., (n.d.).
[36] Zili L, Ben Nasrallah S. Heat and mass transfer during drying in cylindrical packed beds. Numer Heat Transfer Part A: Applic 1999;36(2):201–28.
[37] Sahimi M. Flow and transport in porous media and fractured rock-from classical methods to modern approaches. Dispersion in porous media, Chapter 9. Printed in the federal Republic of Germany; 1995, p. 215–60., (n.d.).
[38] Hunt ML, Tien CL. Non-darcian convection in cylindrical packed beds. ASME J Heat Transfer 1988;110(2):378–84.
[39] Ranz WE. Friction and transfer coefficients for single particles and packed beds. J Chem Eng Prog 1952;48(5):247–53, (n.d.).

[40] Ahmed MH, Kattab NM, Fouad M. Evaluation and optimization of solar desiccant wheel performance. Renew Energy 2005;30:305–25. https://doi.org/10.1016/j.renene.2004.04.010.
[41] Sakoda A, Suziki M. Simultaneous transport of heat and mass in closed type adsorption cooling system utilizing solar heat. J Sol Energy Eng ASME 1986;108:239–90, (n.d.).
[42] Kodama A, Hirayama T, Goto M, Hirose T, Critoph RE. The use of psychrometric charts for the optimisation of a thermal swing desiccant wheel. Appl Therm Eng 2001;21:1657–74. https://doi.org/10.1016/S1359-4311(01)00032-1.
[43] Chua HT, Ng KC, Malek A, Kashiwagi T, Akisawa A, Saha BB. Modeling the performance of two-bed, silica gel-water adsorption chillers. Int J Refrig 1999;22:194–204. https://doi.org/10.1016/S0140-7007(98)00063-2.
[44] Mtimet I, Zili-Ghedira L. Numerical Study of a Desiccant Cooling Installation in Variable Climates. J Por Media 2009;12(12):1237–46.
[45] Angrisani G, Roselli C, Sasso M. Dehumidification and Thermal Behavior of Desiccant Wheels: Correlations Based on Experimental and Manufacturer Data. Heat Transf Eng 2018;39:293–303. https://doi.org/10.1080/01457632.2017.1295743.
[46] Beccali M, Butera F, Guanella R, Adhikari RS. Simplified models for the performance evaluation of desiccant wheel dehumidification. Int J Energy Res 2003;27(1):17–29.
[47] Puglisi G, Morosinotto G, Emmi G. Development of an advanced simulation model for solar cooling plants. Energy Procedia 2015;70:495–503. https://doi.org/10.1016/j.egypro.2015.02.153.
[48] Visek E, Mazzrella L, Motta M. Performance analysis of a solar cooling system using self tuning fuzzy-PID control with TRNSYS. Energy Procedia 2014;57:2609–18. https://doi.org/10.1016/j.egypro.2014.10.272.
[49] R.U. Rony, H. Yang, S. Krishnan, J. Song, Recent advances in transcritical CO 2 (R744) heat pump system: A review, 2019. doi: 10.3390/en12030457.
[50] Sarkar J, Bhattacharyya S, Gopal MR. Optimization of a transcritical CO2 heat pump cycle for simultaneous cooling and heating applications. Int J Refrig 2004;27:830–8. https://doi.org/10.1016/j.ijrefrig.2004.03.006.
[51] ASHRAE. 15 & 34 Safety Standard for Refrigeration Systems and Designation and Classification of Refrigerants ISO 5149 Mechanical Refrigerating Systems Used for Cooling and Heating—Safety Requirements. Available online: https://www.ashrae.org/technical-res, (n.d.).
[52] Lorentzen G, Pettersen J. A new, efficient and environmentally benign system for car air-conditioning. Int J Refrig 1993;16(1):4–12.
[53] Riffat SB, Afonso CF, Oliveira AC, Reay DA. Natural refrigerants for refrigeration and air-conditioning systems. Appl Therm Eng 1997;17:33–42. https://doi.org/10.1016/1359-4311(96)00030-0.
[54] Lorentzen G. Revival of carbon dioxide as a refrigerant. Int J Refrig 1994;17(5):292–301.
[55] Sarkar J. Review on cycle modifications of transcritical CO2 refrigeration and heat pump systems. J Adv Res Mech Eng 2010;1:22–9.
[56] F.S. Trg-trc, Clinic Cooling and Heating Cooling and Heating, (n.d.).
[57] No Title, (n.d.). https://www.engineeringtoolbox.com/velocities-ventilation-ducts-d_211.html.
[58] Governo, Descrizione dell'edificio di riferimento e parametri di Verifica - Appendice A, (2015) 1–8.
[59] Jia CX, Dai YJ, Wu JY, Wang RZ. Use of compound desiccant to develop high performance desiccant cooling system. Int J Refrig 2007;30:345–53. https://doi.org/10.1016/j.ijrefrig.2006.04.001.
[60] Liu Y, Meng D, Sun Y. Feasible study on desiccant wheel with CO2 heat pump. IOP Conf Ser Earth Environ Sci 2017;100:012209.
[61] PVGIS, (n.d.). https://re.jrc.ec.europa.eu/pvg_tools/en/.
[62] Dai B, Qi H, Liu S, Zhong Z, Li H, Song M, et al. Environmental and economical analyses of transcritical CO2 heat pump combined with direct dedicated mechanical subcooling (DMS) for space heating in China. Energy Convers Manag 2019;198. https://doi.org/10.1016/j.enconman.2019.01.119.
[63] Eicker U, Pietruschka D. Optimization and economics of solar cooling systems. Adv Build Energy Res 2009;3:45–81. https://doi.org/10.3763/aber.2009.0303.
[64] P.D. (2022). W.P.P. 2022: S. of R. United Nations Department of Economic and Social Affairs, World Population Prospects 2022, 2022. www.un.org/development/desa/pd/.
[65] Kaito C, Ito A, Kimura S, Kimura Y, Saito Y, Nakada T. Topotactical growth of indium sulfide by evaporation of metal onto molybdenite 2000;218(2-4):259–64.
[66] Environmental Protection Agency, Landfill Gas Energy Project Development Handbook. Chapter 4. Project Economics and Financing, (2021). https://www.epa.gov/lmop/landfill-gas-energy-project-development-handbook.
[67] Zhang Q, Liu X, Zhang T, Xie Y. Performance optimization of a heat pump driven liquid desiccant dehumidification system using exergy analysis. Energy 2020;204:117891. https://doi.org/10.1016/j.energy.2020.117891.
[68] Kim E, Lee J, Jeong Y, Hwang Y, Lee S, Park N. Performance evaluation under the actual operating condition of a vertical ground source heat pump system in a school building. Energ Build 2012;50:1–6. https://doi.org/10.1016/j.enbuild.2012.02.006.
[69] P. It, Control strategies of open cycle desiccant cooling systems minimising energy consumption. Stéphane Ginestet, Pascal Stabat, Dominique Marchio, Centre d ' énergétique (Cenerg) Ecole des Mines de Paris, (2001).